Tissue Eng Regen Med (2021) 18(2):279–295
https://doi.org/10.1007/s13770-020-00309-w

Online ISSN 2212-5469

ORIGINAL ARTICLE

The Therapeutic Potential of Amniotic Fluid-Derived Stem Cells on Busulfan-Induced Azoospermia in Adult Rats

Heba F. Ibrahim[1] · Safinaz H. Safwat[1] · Teshreen M. Zeitoun[1] · Khaled F. El Mulla[2] · Amira Y. Medwar[1]

Received: 22 July 2020 / Revised: 20 September 2020 / Accepted: 13 October 2020 / Published online: 13 March 2021

Abstract

BACKGROUND: Busulfan is an alkylating chemotherapeutic agent that is routinely prescribed for leukemic patients to induce myelo-ablation. However, it also results in azoospermia and infertility in cancer survivors. This research was constructed to explore the possible therapeutic role of amniotic fluid-derived stem cells (AFSCs) in improving busulfan-induced azoospermia in adult rats.

METHODS: Forty two adult male albino rats were randomized into: (1) control group, (2) azoospermia group, (3) spontaneous recovery group, and (4) AFSCs-treated group, in which AFSCs were transplanted through their injection into the testicular efferent ducts. The assessment included a histo-pathological examination of the seminiferous tubules by the light and transmission electron microscopes. Additionally, the confocal laser scanning microscope was used for confirmation of homing of the implanted cells. Moreover, we conducted an immuno-fluorescence study for detection of the proliferating cell nuclear antigen (PCNA) in the spermatogenic cells, epididymal sperm count, and a histo-morphometric study.

RESULTS: AFSCs successfully homed over the basement membrane of the injured seminiferous tubules. They greatly attenuated busulfan-induced degenerative and oxidative changes. They also caused a re-expression of PCNA in the germ cells, leading to resumption of spermatogenesis and re-appearance of spermatozoa.

CONCLUSION: AFSCs could be a promising treatment modality for male infertility induced by chemotherapy, as they possess prominent regenerative, anti-apoptotic, and anti-inflammatory potentials.

Keywords Amniotic fluid-derived stem cells · Busulfan · Azoospermia · Efferent ducts

1 Introduction

Over the past half a century, survival rates from cancer have improved dramatically. These high cure rates are associated with several long-term sequelae of cancer and its treatment. Unfortunately, male infertility is a major one of chemotherapy drawbacks, and preservation of cancer patient's fertility has become a critical healthcare issue [1].

Busulfan is a common alkylating chemotherapeutic drug. It is used as a myeloablative agent in the conditioning regimens before hematopoietic cell transplantation for patients suffering from chronic myeloid leukemia [2]. However, it exhibits severe adverse effects on all other

✉ Heba F. Ibrahim
drhebafathy@yahoo.com

[1] Department of Histology and Cell Biology, Faculty of Medicine, Alexandria University, Dr Fahmi Abdelmeguid St., Al. Mowassat Campus, Alexandria 21561, Egypt

[2] Department of Dermatology, Venereology and Andrology, Faculty of Medicine, Alexandria University, Alexandria 21514, Egypt

cells characterized by a physiological high proliferation rate, including the testicular germ cells, up to their eradication and induction of azoospermia [1, 3].

Stem cells seem to dominate the next frontier of regenerative medicine, owing to their indefinite self-renewal, potential to differentiate into other types of cells, and the fact that, our endogenous repair mechanisms already depend on stem cells residing in different tissues [4].

Recently, amniotic fluid-derived stem cells (AFSCs) have gained a lot of attention to be used as cell therapy. They display the whole criteria of the adult mesenchymal stem cells (MSCs). Additionally, they harbor a subpopulation that expresses several pluripotency markers, just as the embryonic stem cells (ESCs). Subsequently, AFSCs represent a new class of stem cells with an intermediate phenotype, residing in-between the adult and the ESCs. They could differentiate into cells belonging to the three germ layers without being tumorigenic. These advantageous characteristics, together with absence of ethical issues concerning their obtainment, have highlighted their potential role in regenerative medicine [5, 6].

In the present study, we aimed at assessing the histopathological changes of the seminiferous tubules of adult male albino rats, following induction of azoospermia by busulfan. Furthermore, exploring the presence of a possible therapeutic role of AFSCs in improving busulfan-induced azoospermia.

2 Materials and methods

2.1 Isolation and culture of AFSCs

Five pregnant females Sprague Dawley albino rats (aged about 6–8 weeks, with an average body weight of 150–200 g), were used to obtain the amniotic fluid samples. Rats were euthanized by an over dose of ether, at day 11.5 of pregnancy [7]. Aseptically, the gestational sacs were excised and soaked in 70% ethanol in a sterile Petridish for 2 min, and then transferred to phosphate buffered saline (PBS, Lonza, Switzerland) in another sterile Petridish, for rinsing off the ethanol [8]. Amniotic fluid was then collected from the sacs, using 30-gauge needles, and centrifuged at 1400 rounds per minute for 10 min, then the pellet was re-suspended in 5–10 ml of complete culture medium (CCM), prepared as; 1.0 g/L low glucose Dulbecco's modified Eagle's medium (LG-DMEM, Lonza, Switzerland), 10% Fetal Bovine Serum (FBS, Hyclone, Logan, UT, USA), 2 mM L-glutamine, and 1% penicillin/streptomycin (10.000 IU/ml/10.000 µg/ml, Lonza, Switzerland) [9, 10].

The cells suspension was then transferred to a vented sterile T25 cm^2 tissue culture flask, and cultured at 37 °C in a humidified atmosphere, with 5% CO_2. After 72 h, the non-adherent cells were washed away by a pre-warmed PBS, and the culture medium was changed. Later, medium was changed once every 2–3 days [10].

When the primary cultured cells reached 80–90% confluent, they were detached by adding 1 ml of 0.25% trypsin–EDTA solution (170.000 U/l–200 mg/L), and reseeded in CCM at a splitting ratio 1:3 [11]. The cells were counted by the hemocytometer under the phase contrast inverted microscope (Olympus CKX41SF, Japan), and their viability was assessed by the trypan blue exclusion test [12]. Passage 3 cultured cells were used in the current experiment.

2.2 Characterization of AFSCs

2.2.1 Morphological characterization

The cultured cells were monitored daily and characterized morphologically using the phase-contrast inverted microscope [13].

2.2.2 Characterization by colony-forming unit-fibroblast (CFU-F) assay

For assessing the proliferation and the clonogenic capacities of the cells, 100 AFSCs from passage 3, were cultured in 10 ml of CCM, in a 100 mm diameter dish, for 14 days, with a half-weekly medium changing. On day 14, the medium was discarded and the cells were washed with PBS. To visualize colonies, the cells were fixed, stained by 3% crystal violet stain (Sigma–Aldrich, St. Loise, MO, USA), and examined by the phase contrast inverted microscope. The colony forming unit (CFU) potential = number of colonies that were formed/ number of cells that were plated X100 [14].

2.2.3 Characterization by fluorescence-activated cell sorting (FACS)

The surface markers of passage 3 AFSCs were characterized using fluorescent-labeled monoclonal antibodies. Cells were trypsinized, washed with PBS, and incubated for 30 min, in the dark, with monoclonal Allophycocyanin-conjugated antibody for CD90, monoclonal phycoerythrin-conjugated antibody for CD45, and monoclonal fluorescein isothiocyanate-conjugated antibody for OCT-4 (Abcam, Cambridge, UK). Immuno-fluorescence of the viable cells was performed using FACS caliber flow cytometer, equipped with Cell Quest Software (Becton, Dickinson and Company, Franklin Lakes, NJ, USA) [9, 11].

2.2.4 Labeling of AFSCs for tracing

AFSCs were labeled with the florescent Cell Tracker CM-Dil (Invitrogen, Cergy Pontoise, France, excitation/ emission wave lengths 549/565 nm). It was supplied as a ready-made cell-labeling solution (50 µg/vial). For preparing a stock solution, 50 µl of dimethyl sulfoxide (DMSO) was added, and the vial was stored at − 20 °C. For preparing a working solution, 10 µg of the stock solution were diluted in 10 ml PBS. Following that, AFSCs in CCM were incubated in the working solution for 7 min at 37 °C, and for additional 15 min at 4 °C. Cells were then centrifuged, and the labeled pellets were re-suspended in fresh CCM [15]. For detection of the efficacy of labeling, about 50,000 labeled AFSCs in CCM, were fixed on a cover slip by 4% formaldehyde for 10 min, washed twice by PBS, each for 3 min, and examined by the confocal laser scanning microscope (Leica TSC SPE II/ DMi 8, Mannheim, Germany) [16].

2.3 The experimental design

Forty-two adult male Sprague–Dawley albino rats, weighing 200–250 g, at 8–12 weeks of age, were used. Each rat had a free access to water and standard rodent soft chow. Rats were handled in a strict accordance with the institutional guidelines for care and use of laboratory animals. The experimental rats were randomly divided into four groups:

1) The control group: 10 rats, each received a single intra-peritoneal (IP) injection of PBS.
2) The azoospermia group: 10 rats, each received a single IP injection of 40 mg/kg busulfan [17]. It was obtained from the Bone Marrow Transplantation unit of Al-Mowassat Campus, University of Alexandria. Rats were euthanized by cervical dislocation under ether anesthesia after 28 days [18].
3) The spontaneous recovery group: 10 rats, each received a single IP injection of 40 mg/kg busulfan, and then were euthanized after 56 days.
4) The AFSCs-treated group: 12 rats, each received a single IP injection of 40 mg/kg busulfan. After 28 days, about 1×10^6 labeled AFSCs were suspended in 1 ml CCM, and loaded into a 1 ml syringe. Each rat was anesthetized by intramuscular injection of ketamine (50 mg/kg) and xylazine (5 mg/kg), then a 1 cm midline abdominal incision was done to expose the peritoneal cavity. Each testis was exteriorized, and the site of the efferent ducts was identified and lifted on a forceps. By applying a pressure to the syringe loaded with the AFSCs, its content was gently forced into the seminiferous tubules through a retrograde injection into the efferent ducts. After the content was completely injected, each testis was returned to the abdominal cavity, and the abdominal wall and skin were sutured [19].

   Homing of the transplanted labeled cells within the seminiferous tubules was confirmed by excision of testes of two randomly selected rats of AFSCs-treated group, 48 h after transplantation. Testicular tissues were fixed, processed to get unstained 5 µm thick paraffin sections, mounted on poly (L-lyse)-coated glass slides, deparaffinized, rehydrated, and examined by the confocal microscope [20]. The remaining 10 rats of AFSCs-treated group were euthanized after another 28 days.

2.4 Histological and immuno-fluorescence studies

2.4.1 Histological study

At the specified times of the experiment, each testis was cut into 2 specimens; the first specimen was fixed in Bouin's solution, processed to get 5 µm thick paraffin sections [21]. The second specimen was cut into small pieces (0.5–1 mm^3) and immediately fixed in 3% phosphate buffered glutaraldehyde solution [22].

2.4.1.1 Light microscopic study The deparaffinized 5 µm thick sections were stained with hematoxylin and eosin (H&E), mounted on glass slides, and examined by the light microscope (BX41, Olympus Tokyo, Japan) [21]

2.4.1.2 Electron microscopic study The small pieces (0.5–1 mm^3) were post-fixed in 1% osmium tetroxide, rinsed in phosphate buffer for 1–2 h, dehydrated with graded ethanol, embedded in plastic capsules of araldite, polymerized, and processed to get ultra-thin sections (80 nm thick). The sections were then mounted on copper grids, stained with uranyl acetate for 20 min, followed by lead citrate for 10 min, and examined by the transmission electron microscope (JEOL-JSM 1400 Plus, Tokyo, Japan) [22].

2.4.2 Immuno-fluorescence study

Deparaffinized 5 µm thick testicular sections mounted on poly-L-lysine-coated glass slides were rehydrated, rinsed in deionized water, and immersed for 10 min in a wash buffer supplied with the antibody kit. Then, the sections were washed 3 times for 5 min each, with TBS (PBS + 0.1% Triton X-100), and blocked with 1% bovine serum albumin (BSA) in TBS, for 1 h, at room temperature [23]. The slides were incubated overnight at 2–8 °C with mouse anti-proliferating cell nuclear antigen (PCNA) primary

antibodies, diluted in TBS with 1% BSA. Next, they were rinsed with the wash buffer, 3 times for 5 min each, then incubated for 60 min, at room temperature, in the dark, with goat anti-mouse secondary antibodies, conjugated with Alex Fluor 555 (Invitrogen, Cat # A-21422; excitation/emission wave lengths 555/580 nm), and diluted in TBS with 1% BSA. Immuno-stained sections were examined by the confocal microscope. All reactions were performed using appropriate positive and negative controls [23, 24].

2.5 Epididymal sperm count and histo-morphometric study

2.5.1 Epididymal sperm count

Each cauda epididymis of the rats was excised and minced using a sharp scissor in a pre-warmed Petri-dish containing 1 ml of PBS (pH 7.4) at 37 °C. The spermatozoa were allowed to disperse for 20–25 min in the incubator. Then, a spermatozoal suspension was prepared by several times of re-pipetting, and 0.05 ml of each suspension was placed on a clean glass slide, examined by the light microscope (Mic. Mag. X100). Sperms were counted in ten non overlapping fields from each slide, and the obtained data was fed to and analyzed by the Computer Assisted Semen Analysis Software (Mira-9000 CASA, Alrubaidi Medical Corporation, Sanaa, Yemen), to get the average sperm count of each epididymis [25].

2.5.2 Histo-morphometric study

NIH Fiji© software program (version 1.51 k, Wayne Rasband, National Institutes of Health, Bethesda, MD, USA), was used to measure:

1) The seminiferous tubular diameter: for each group, 25 transverse sections of the seminiferous tubules from different non-overlapping H&E fields (Mic. Mag. X100), were assessed. Only circular or near circular tubules were chosen. The mean tubular diameter (T) for each tubule, was derived by taking the average of two diameters (T1,T2), which were at right angle to each other [26].
2) The height of the seminiferous epithelium: the luminal diameter (L) for each chosen seminiferous tubule, was derived by taking the average of two diameters (L1, L2), which were at right angle to each other. The average height of the seminiferous epithelium (H) for each tubule was calculated according to the equation: H = T−L [26].
3) The intensity of fluorescence of PCNA: for each group, the intensity of fluorescence was measured in ten different non-overlapping fields/ five immuno-stained sections with anti PCNA antibodies (confocal microscope, Mic. Mag. X630) [27].

2.6 Statistical analysis

Data concerning the mean intensity of fluorescence of PCNA, the mean epididymal sperm count, the mean diameter of the seminiferous tubules, and the mean height of the germinal epithelium, was fed to the computer and analyzed, using the statistical package for social sciences (SPSS, version 20; IBM, Chicago IL, USA) software package. One-way ANOVA test was used to compare between the different groups, followed by a post hoc test (Tukey) for the pair-wise. The results were presented as the mean ± SD. $p < 0.05$ was considered statistically significant [28].

3 Results

3.1 Characterization of AFSCs

When examined by the phase contrast inverted microscope, 72 h after seeding, some AFSCs were adherent to the culture plate, and appeared spindle or flat polygonal in shapes. Some other cells retained their rounded shape as they were still not attached (Fig. 1A). On day 5, the adherent cells appeared fibroblast-like in shape. Other cells were rounded and floating to undergo mitosis (Fig. 1B). The cellular morphology and proliferative potential were maintained, till reaching 80–90% confluency of passage 3 (Fig. 1C).

The CFU-F assay demonstrated a marked clonogenic and proliferative capacities of the cultured AFSCs, indicated by their aggregation into separate islands (colonies), that were identified by crystal violet stain (Fig. 1D). The calculated CFU potential revealed that; each 100 AFSCs, gave about 83% ± 2.32 colonies within 14 days of culturing.

The FACS analysis of passage 3 AFSCs demonstrated that, about 35.65% of the cells were positive for the pleuripotency marker Oct-4 (Fig. 2A), about 85.12% of the cells expressed the mesenchymal marker CD90, and only about 5.58% of the cells were positive for the hematopoietic marker CD45 (Fig. 2B).

3.2 Labeling and homing of AFSCs

The cells have successfully taken up the fluorochrome and exhibited the red fluorescence of CM-Dil in their cytoplasm, as proved by the confocal microscopic examination (Fig. 3A). After 48 h of transplantation, the labeled cells

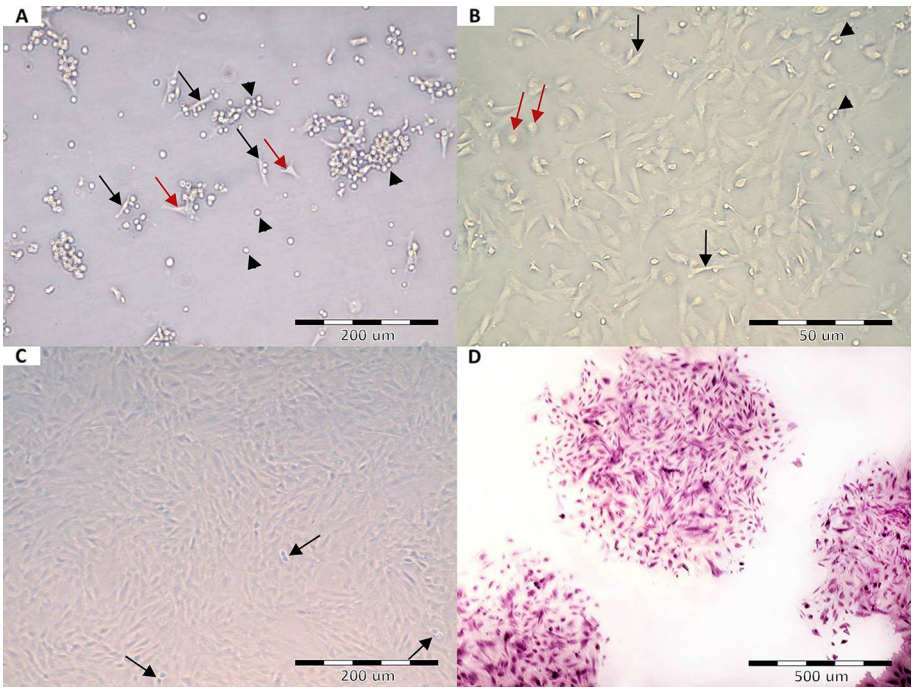

Fig. 1 **A** Passage zero AFSCs after 72 h of cultivation, showing some adherent cells, with either spindle (black arrows) or flat polygonal (red arrows) shapes. The majority of the cells are still not attached to the culture flask (arrowheads). **B** Passage zero after culturing for 5 days, showing dispersed fibroblast-like adherent cells (black arrows), small rounded floating cells (red arrows), and mitotic cells (arrowheads). **C** Passage 3 at 80–90% confluency. Arrows; mitotic cells. **D** Crystal violet-stained colonies. [Phase contrast inverted microscope, Original magnification; **A**, **C** X100, **B** X200, **D** X40]

homed within the germinal epithelium, rather than being floating in the seminiferous tubules lumina (Fig. 3B).

3.3 Histological results

3.3.1 Light microscopic results

3.3.1.1 ***The control group histology*** The control light microscopic examination revealed multiple cross sections of seminiferous tubules with regular outlines. The interstitial spaces were occupied by clusters of interstitial cells "of Leydig" (Fig. 4A). Each tubule was surrounded by regular basement membrane and myoid cells with flattened nuclei, and was lined by Sertoli cells and stratified layers of spermatogenic cells (Fig. 4B).

3.3.1.2 ***Busulfan induced degenerative changes in the azoospermia group*** In the azoospermia group, the seminiferous tubules appeared with disrupted architecture and thickened irregular basement membrane. The tubules were occupied by large vacuolar spaces and dispersed eosinophilic thread-like structures. No spermatozoa could be detected in almost all the tubules. Inter-tubular amorphous eosinophilic exudate was obvious (Fig. 4C, D). Many tubules appeared with a nearly total loss of the germ cells, exhibiting only scattered disorganized Sertoli cells. Few tubules appeared with a reduced thickness of their seminiferous epithelium, retaining some spermatogenic cells with darkly-stained nuclei (Fig. 4D).

3.3.1.3 ***The degenerative signs persisted in the group left for a spontaneous recovery*** In the spontaneous recovery group, the light microscopic examination, revealed small sized seminiferous tubules, containing vacuoles and eosinophilic thread-like material. They were surrounded by a thickened basement membrane. Widening of the inter-tubular spaces and increased cellularity of the interstitial tissue, were noticed (Fig. 4E, F). The seminiferous epithelium showed scattered Sertoli cells, while germ cells were hardly seen (Fig. 4F).

3.3.1.4 ***Rescue of the seminiferous tubules by the AFSCs*** In the AFSCs-treated group, most of the tubules appeared with a more or less normal looking architecture. They were lined by several rows of the different germ cells, and Sertoli cells were seen resting on the basement membrane. Other tubules showed few layers of spermatogenic cells, with minute vacuolar spaces in-between. Few tubules in this group were still small sized and depleted of their germ cells (Fig. 4G, H).

3.3.2 Electron microscopic results

3.3.2.1 ***Control group ultrastructure*** The control seminiferous tubules were surrounded by regular basal lamina and flattened myoid cells. The Sertoli cells appeared elongated with large basally located indented nuclei, and intact inter-Sertoli junctions (Fig. 5A). Spermatogonia (Fig. 5B) and primary spermatocytes (Fig. 5A), were also recognized. Early spermatids appeared with spherical

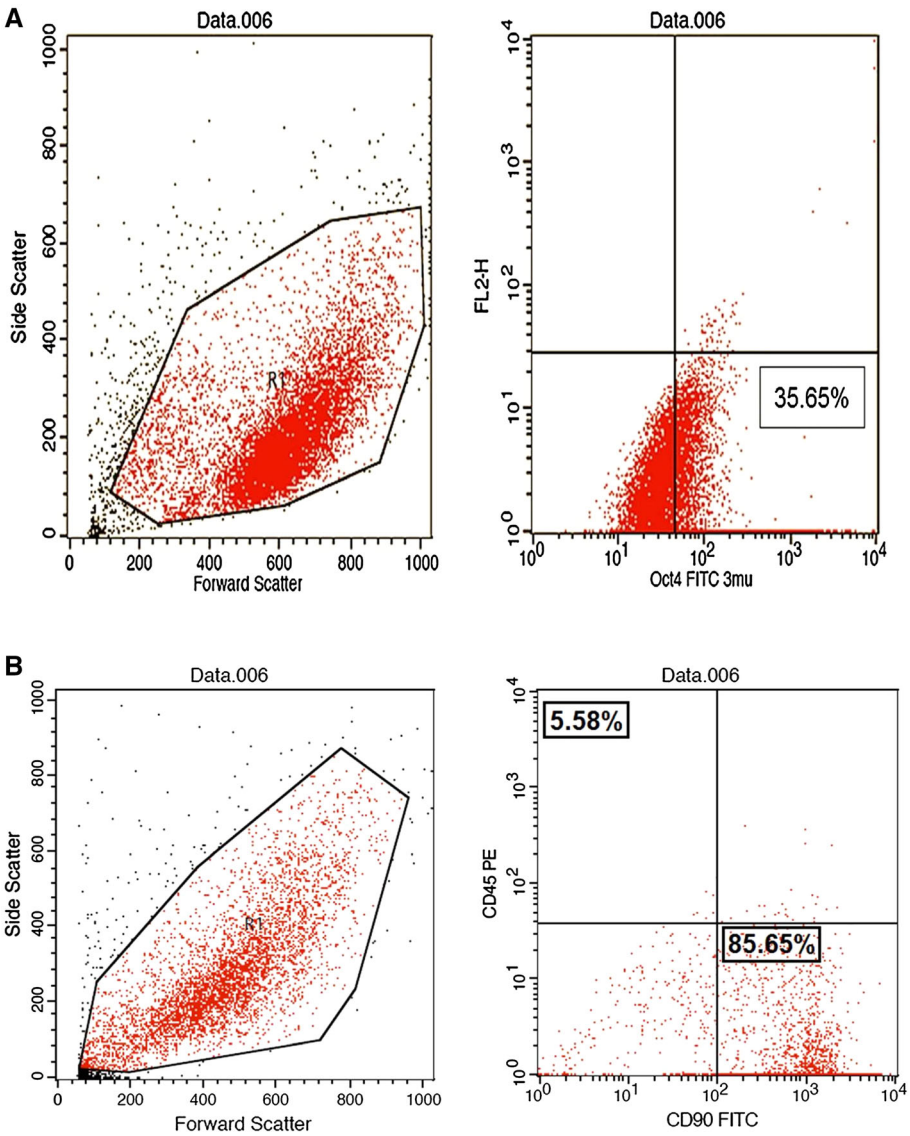

Fig. 2 **A, B** Representative flow cytometric analysis of the cell-surface markers of AFSCs at passage 3

nuclei and abundant peripherally-arranged ring-shaped mitochondria (Fig. 5C). Different cut sections of the spermatozoa were observed (Fig. 5D).

3.3.2.2 ***The azoospermia group exhibited ultrastructural toxic effects of busulfan*** Examination of the ultrathin sections of the azoospermia group, demonstrated seminiferous tubules bounded by irregular thickened basal lamina (Fig. 5E–G), with distorted corkscrew-shaped myoid cells (Fig. 5G). Most of the tubules revealed only Sertoli cells, that appeared disorganized and clumped over each other (Fig. 5E), with large numerous lysosomes (Fig. 5E, F) and rarified cytoplasm (Fig. 5F). Junctional complexes were frequently disoriented and thinned out (Fig. 5E, F). Some spermatogonia exhibiting dilated perinuclear cisterna, were surrounded by wide intercellular spaces (Fig. 5G). The primary spermatocytes appeared shrunken or with irregular outlines (Fig. 5F). Spermatozoa in whatever stage of maturation were not detected.

3.3.2.3 ***Failure of spontaneous recovery ultrastructurally*** The spontaneous recovery group showed that, most of the tubules were surrounded by thickened highly folded basal lamina, and lined by detached Sertoli cells, with rarified cytoplasm (Fig. 5H).

3.3.2.4 ***Improvement of the ultrastructure of the seminiferous tubules by AFSCs*** In the AFSCs-treated group, the majority of the tubules exhibited normal architecture and stratification of the seminiferous epithelium. Sertoli cells, resting on regular basal lamina of an ordinary thickness, appeared with nearly normal ultrastructure and configuration, with apparently intact inter-Sertoli junctions. All types of the spermatogenic cells and several

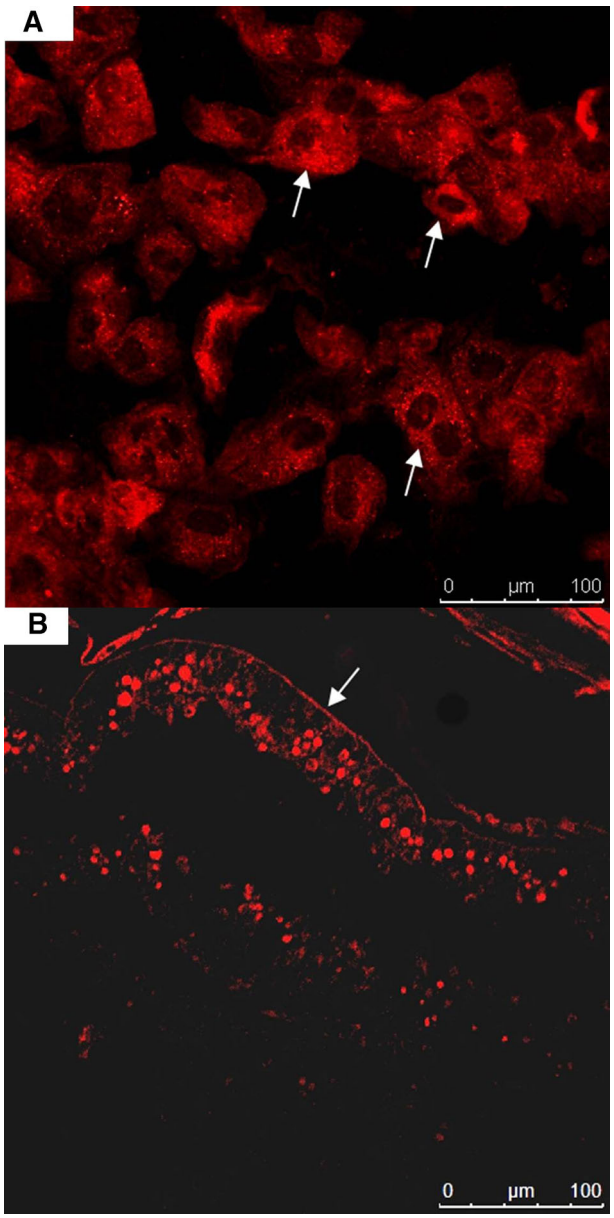

Fig. 3 **A** The cultured cells are expressing CM-Dil red fluorescence in their cytoplasm (arrows). **B** The labeled transplanted cells homed within the seminiferous epithelium. Arrow; non-specific auto-fluorescence of the basement membrane. [Confocal laser scanning microscope, Original magnification X200, scale bar 100, pinhole diameter 94.3 µm]

spermatozoal cut sections were detected (Fig. 6A, B). On the other hand, some partially regenerated tubules in this group exhibited wide intercellular spaces, Sertoli cells with dilated sER, and spermatocytes with disrupted cell membrane (Fig. 6C). A number of spermatozoa showed heads with electron lucent nuclei (Fig. 6D), and middle pieces with vacuolated excess cytoplasm and less-organized mitochondrial sheathes (Fig. 6E). Other few seminiferous tubules were still degenerated, with highly vacuolated Sertoli cells and spermatocytes with dilated perinuclear cisterna (Fig. 6F).

3.4 Immuno-fluorescence microscopic results

Testicular sections from the control group revealed the normal PCNA expression in the spermatogenic cells occupying the outer zone of each tubule, with no detected immuno-reaction in the luminal zone (Fig. 7A). Sections from the azoospermia group revealed a markedly reduced immuno-reaction of PCNA. Some seminiferous tubules exhibited only few scattered immuno-positive spermatogenic cells (Fig. 7B, C). Faint PCNA immuno-fluorescence was detected in the spontaneous recovery group (Fig. 7D). Regarding AFSCs-treated group, there was a variability in the immuno-reactivity, where many tubules revealed fluorescence of PCNA almost similar to the control pattern (Fig. 7E), while other tubules exhibited reduced or weak immuno-reaction (Fig. 7F, G).

Statistically, the intensity of fluorescence of PCNA decreased significantly in the azoospermia and spontaneous recovery groups, in comparison with the control group. In AFSCs-treated group, the decrease was not significantly comparable to that of the control group (at $p \leq 0.05$) (Fig. 7H).

3.5 Epididymal sperm count

There was a significant decrease in the count of the epididymal sperms in all groups, in comparison with the control group. However, AFSCs-treated group showed a significant increase in the sperm count, compared to the azoospermia and spontaneous recovery groups ($p \leq 0.05$) (Fig. 8A).

3.6 Histo-morphometric results

The seminiferous tubular diameter was not significantly different in the azoospermia and AFSCs-treated groups, in comparison with the control group. It decreased significantly only in the spontaneous recovery group ($p \leq 0.05$) (Fig. 8B).

The height of the seminiferous epithelium showed a significant decrease in all groups, in comparison with the control group. However, it showed a significant increase in AFSCs-treated group, in comparison with the azoospermia and spontaneous recovery groups ($p \leq 0.05$) (Fig. 8C).

4 Discussion

In the current work, the induction of azoospermia by busulfan, was confirmed by the remarkable loss of all series of differentiating germ cells, that were replaced by large

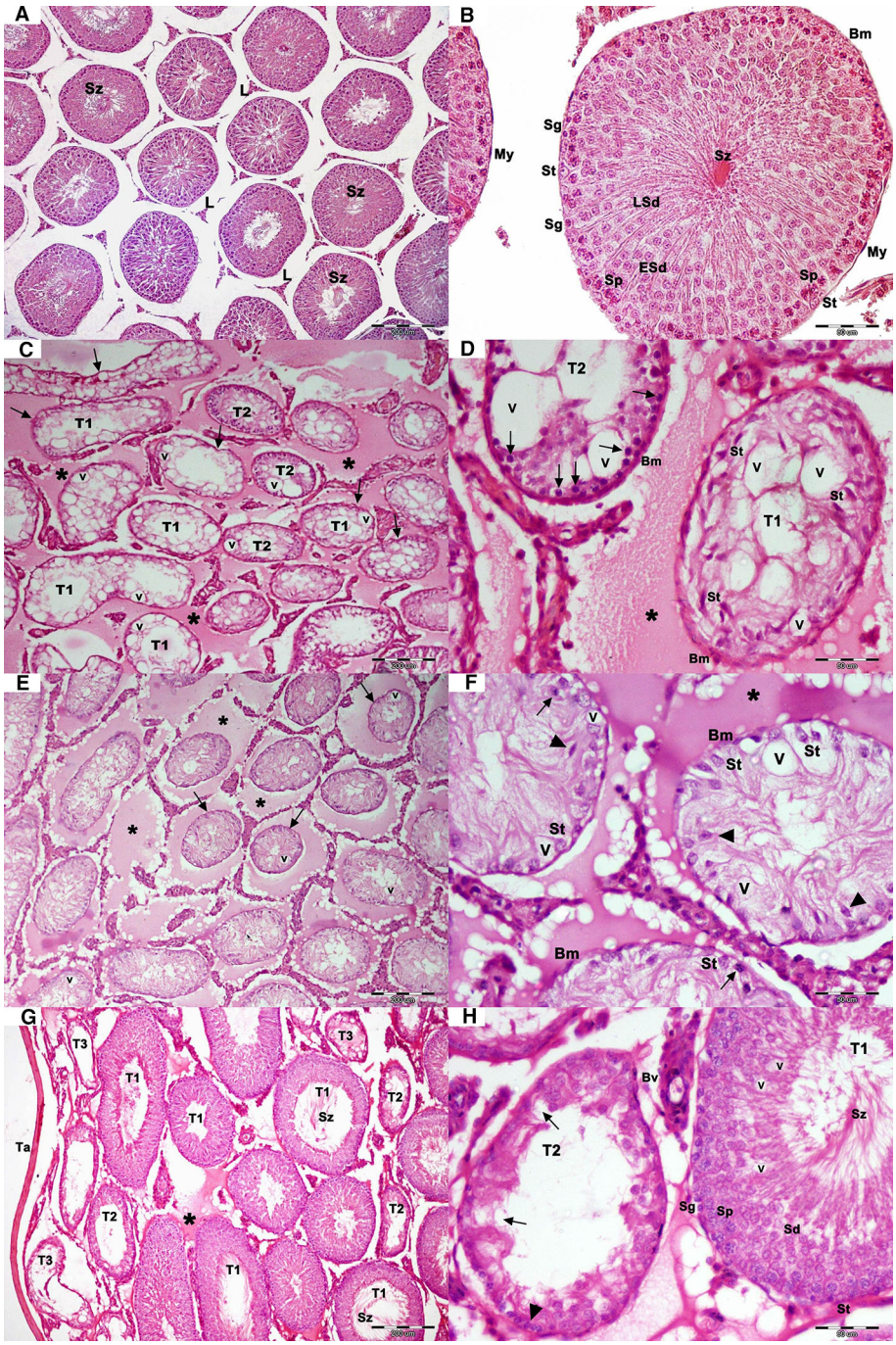

Fig. 4 Seminiferous tubules light microscopic assessment. **A**, **B** Regular cross sections of the seminiferous tubules, surrounded by regular basement membrane (Bm), and lined by Sertoli cells (St) and the different spermatogenic cells. *L*; interstitial cells "of Leydig", *Sg*; spermatogonia, *Sp*; primary spermatocytes, *ESd*; early spermatids, *LSd*; late spermatids, *Sz*; spermatozoa, *My*; myoid cells. **C** Most of the tubules (T1) appear depleted of the spermatogenic cells, with irregular outlines (arrows). Other tubules (T2) appear with some spermatognic cells. **D** The tubule (T1) shows detached and disorganized Sertoli cells (St), while (T2) shows few rows of spermatogenic cells with darkly stained nuclei (arrows). Notice the thickened basement membrane (Bm). **E** Non spermatogenic small sized seminiferous tubules (arrows) are seen. **F** The tubules show scattered Sertoli cells (St), some of their nuclei (arrowheads) are seen away from the thickened basement membrane (Bm). Notice the few germ cells with darkly stained nuclei (arrows) and the increased cellularity of the interstitial tissue. **G**, **H** Some tubules (T1) appear apparently normal. Other tubules (T2) are lined by some spermatogenic cells, with a well-organized row of spermatogonia (arrowhead) and minute vacuolar spaces (arrows). While the tubules (T3) are small sized and depleted of their spermatogenic cells. *Sg*; spermatogonia, *Sp*; primary spermatocytes, *Sd*; spermatids, *Sz*; spermatozoa, *St*; Sertoli cells, *Ta*; tunica albuginea, *Bv*; interstitial blood vessels. [*asterisks*; intertubular amorphous eosinophilic exudate, *V* vacuoles, H&E, scale bar **(A**, **C**, **E**, **G)** 200 μm, and **(B**, **D**, **F**, **H)** 50 μm]

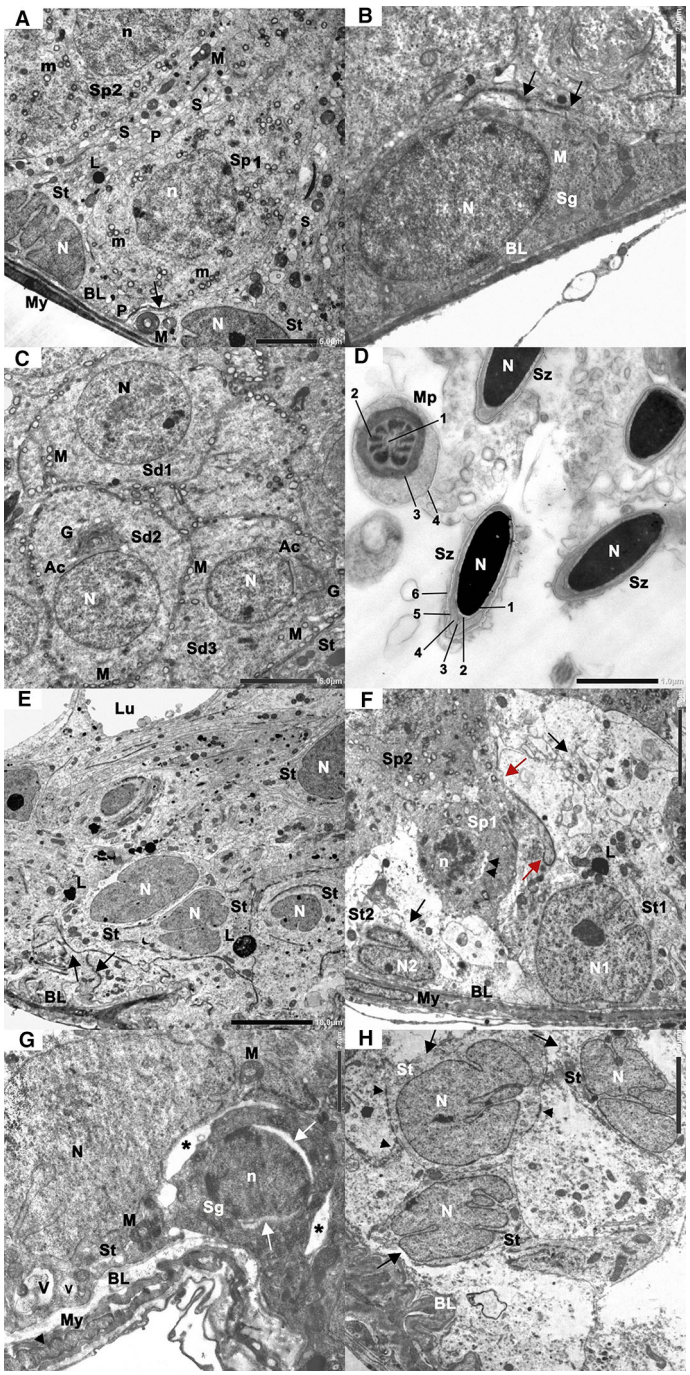
A
n
m
M
Sp2
S
S
P
Sp1
L
St
n
S
N
m
m
BL
My
P
N
St
M
B
M
N
Sg
BL
C
N
M
Sd1
G
Sd2
Ac
Ac
M
N
N
G
M
St
Sd3
M
D
N
Sz
2
Mp
1
3
4
Sz
N
N
Sz
6
5
1
4
3
2
E
Lu
St
N
L
N
St
N
St
St
L
BL
F
Sp2
Sp1
n
L
St2
St1
N2
N1
My
BL
G
M
N
*
n
Sg
M
*
St
BL
V
v
My
H
St
St
N
N
N
St
BL

◀**Fig. 5** Seminiferous tubules electron microscopic assessment. **A** Sertoli cells (St) with indented nuclei (N), are seen resting on regular basal lamina (BL), surrounded by flat myoid cells (My). Primary spermatocytes (Sp1, Sp2) appear with large rounded nuclei (n). *Arrow*; intact junctional complexes, *M*; Sertoli cell mitochondria, *L*; lysosomes; *S*; sER, *P*; Sertoli cell processes, *m*, primary spermatocyte mitochondria. **B** A spermatogonium (Sg) with its nucleus (N) is broadly applied to the basal lamina (BL). *M*; mitochondria, *Arrows*; inter-Sertoli junctions. **C** Several early spermatids (Sd1, Sd2, Sd3), with their rounded nuclei (N), are illustrated. *St*; Sertoli cell, *M*; ring-shaped mitochondria, *G*; Golgi complex, *Ac*; acrosomal cap. **D** Spermatozoal heads (Sz) show very electron dense nuclei (N), that are surrounded by the nuclear membrane (1), subacrosomal space (2), inner acrosomal membrane (3), acrosomal material (4), outer acrosomal membrane (5), and cell membrane (6). In the middle piece (Mp), the axoneme (1) is surrounded by; nine outer dense fibers (2), a regular mitochondrial sheath (3), and flagellar membrane (4). **E** A group of clumped Sertoli cells (St), with disorganized inter-Sertoli junctional complexes (arrows) are seen. *N*; indented nuclei, *L*; large lysosomes, *BL*; thickened irregular basal lamina, *Lu* lumen of the tubule. **F** Two Sertoli cells (St1, St2) with basally located nuclei (N1, N2), showing rarified cytoplasm and areas of disrupted cell membrane (black arrows). The inter-Sertoli junctions are interrupted and thinned out (red arrows). A shrunken primary spermatocyte (Sp1) is also noticed. Its nucleus (n) shows dilated perinuclear cisterna (arrowheads) and electron dense masses of chromatin. Another primary spermatocyte (Sp2) is seen with an irregular outline. *L*; large lysosomes, *BL*; basal lamina, *My*; Myoid cell. **G** A Sertoli cell (St) with its indented nucleus (N) shows some cytoplasmic vacuoles (V). The spermatogonium (Sg) is surrounded by wide intercellular spaces (asterisks). Its nucleus (n) exhibits dilated perinuclear cisterna (arrows). Notice the distorted myoid cell (My), exhibiting a corkscrew-shaped nucleus (arrowhead). *BL*; thickened basal lamina, *M*; mitochondria. **H** A group of detached Sertoli cells (St) with deeply-infolded nuclei (N) and rarified cytoplasm. Their cell membrane is disrupted (arrows) and the inter-Sertoli junctions (arrowheads) are disorganized and thinned out. [BL; thickened highly folded basal lamina, scale bar **(A**, **C**, **F**, **H)** 5 μm, **(B**, **G)** 2 μm, **(D)** 1 μm, and **(E)** 10 μm]

vacuoles and eosinophilic material. This issue was in agreement with several previous studies on busulfan-induced azoospermia [18, 29, 30].

Moreover, the few apparently preserved spermatogonia and spermatocytes appeared with darkly stained nuclei. Nuclear darkening is a sign of cellular apoptotic changes [31]. Busulfan is known to cause apoptosis and destroy the DNA, through alkylation of N7 and O6 of guanine, and N3 of adenine, forming intra-strand crosslinks, with a subsequent increase in p53 expression, leading to induction of the intrinsic pathway of apoptosis [32, 33]. The extrinsic pathway of apoptosis is also activated, through busulfan-induced Fas receptors expression in the germ cells [29]. The enhanced rate of phagocytosis of the apoptotic germ cells explains appearance of Sertoli cells with large sized lysosomes [31]. While, the intratubular eosinophilic structures and large vacuoles that were detected by the light microscope, represent cellular debris and spaces left after the widespread germ cells death [30, 34].

On the other hand, busulfan treatment did not cause a marked degeneration of Sertoli cells. They appeared disorganized and clumped into small aggregates, the result that was in accordance with Qin et al. [35]. This finding could be related to busulfan-induced progressive alteration of Sertoli cells surface markers and cytoskeletal proteins. It could elevate expression of cytokeratin-18, induce collapsing of vimentin, and cause a significant decline in the microtubules motor activity [29, 36].

We also detected interrupted and thinned out inter-Sertoli junctions in the azoospermia group. This is probably due to busulfan-induced loss of the intercellular adhesion molecule-1 (ICAM-1) [37], and several other junctional proteins, such as; connexin-43, cadherin-2, and ZO-1, leading to detachment of both healthy and injured Sertoli cells, from each other and from the basement membrane [38, 39]. Furthermore, the oxidative stress induced by busulfan [37, 40] causes peroxidation and rupture of the cells membranes, impairment of the energy dependent Na^{+}–K^{+} ion pumps, and cells vacuolization, resulting in more disruption of the inter-Sertoli junctions [41].

The oxidative stress causes also an increasing in the deposition of proteoglycans and collagen by Sertoli and myoid cells, as a defense mechanism, leading to the observed thickening of the basement membrane of the seminiferous tubules [42]. While the basement membrane irregularity might be related to the sustained contraction of the myoid cells, that appeared irregular with corkscrew-shaped nuclei, due to a progressive alteration of their desmin and actin proteins [43].

It worth mentioning also that, the noticed inter-tubular amorphous eosinophilic exudate, could be explained by the ability of busulfan to initiate a state of non-infectious endogenous inflammation. It induces expression of tumor necrosis factor-α (TNF-α) and macrophage chemotactic protein-1 (MCP-1) in the testis [44]. This general inflammatory response, together with the increased cellular apoptosis, could interfere with the testicular venous drainage, leading to inter-tubular capillary congestion and exudation [41].

The histological examination of the rats left for a spontaneous recovery, revealed non spermatogenic seminiferous tubules with persistence of the degenerative changes, similar to the azoospermia group, and they even got worse. Previous researches [3, 30] have documented also failure of autonomous tubular recovery by the endogenous repair mechanisms after busulfan administration. This inability of the spermatogonial stem cells to restore homeostasis, proliferate, and differentiate spontaneously is attributed to the unsuitability of the physical microenvironment following chemotherapy. The vacant cell niches have no favorable growth factors/hormonal

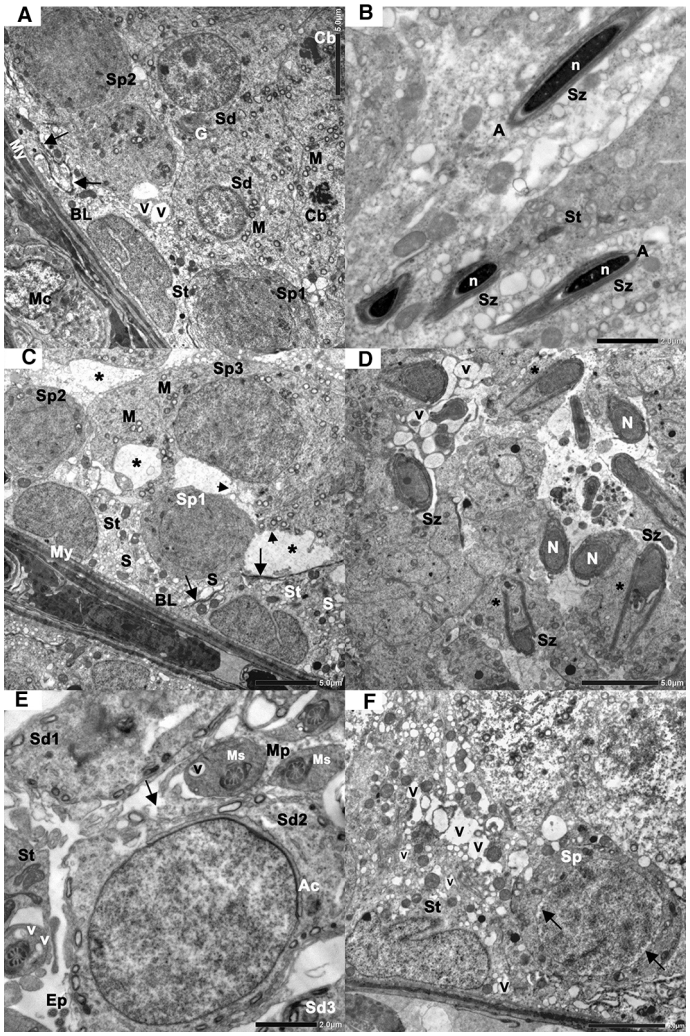

Fig. 6 Electron microscopic assessment of the seminiferous tubules of the AFSCs-treated group **A** An apparently normal looking rat seminiferous epithelium, with intact inter-Sertoli junctions (arrows). *St*; Sertoli cell, *Sp;* primary spermatocytes, *Sd*; early spermatids, *Cb*; chromatoid bodies, *M*; mitochondria, *G*; Golgi complex, *V*; intercellular vacuoles, *Mc*; interstitial macrophage. **B** Normal looking spermatozoa (Sz) with their condensed nuclei (n) and overlying acrosomes (A). *St*; Sertoli cell cytoplasm. **C** Sertoli cells (St) appear with dilated sER (S). The spermatocyte (Sp3) exhibits areas of interrupted cell membrane (arrowheads). Arrows; apparently normal inter-Sertoli junctions, *asterisks*; wide intercellular spaces, *M*; mitochondria, *BL*; basal lamina, *My*; myoid cells. **D** Spermatozoal heads (Sz) with electron lucent nuclei (N) and excess residual cytoplasm (asterisks). *V*; vacuoles. **E** The spermatid (Sd2) appears with a disrupted cell membrane (arrow). The adjacent middle pieces (Mp) exhibit disorganized mitochondrial sheaths (Ms) and excess vacuolated (V) cytoplasm. *Ac*; acrosomal cap, *Ep*; end pieces, *St*; Sertoli cell. **F** A highly vacuolated (V) Sertoli cell (St) and a primary spermatocyte (Sp) with dilated perinuclear cisterna (arrows). [scale bar **(A**, **C**, **E**, **F)** 5 µm, and **(B**, **D)** 2 µm]

milieu, no supporting intact junctions, and no appropriate signaling pathways [45].

Interestingly, we demonstrated a hyper-cellularity of the interstitium in this group. This is explained by persistence of busulfan-induced inflammatory mediators, that act as chemotactic factors, attracting macrophages and other leukocytes, and causing a heavy mononuclear infiltration into the testis [42, 44].

In the present work, we explored the therapeutic potential of AFSCs, as they possess high proliferation rate and differentiation plasticity. In addition, they could be easily obtained, isolated, and expanded [5, 6]. We isolated the cells from the pregnant female rats at day 11.5, according to Wen et al. [7] who documented that, about 70–90% higher success rates in isolation and culture of AFSCs, could be achieved during the middle gestational stage of rats pregnancy.

Immuno-phenotyping of passage 3 cultured AFSCs in our study, demonstrated that, they were positive for the surface marker CD 90, thus they follow the criteria of the adult MSCs. A subpopulation of them were positive for Oct-4, confirming that, AFSCs can be considered pluripotent-like stem cells. They were negative for CD 45, accordingly they do not belong to the hematopoietic cell

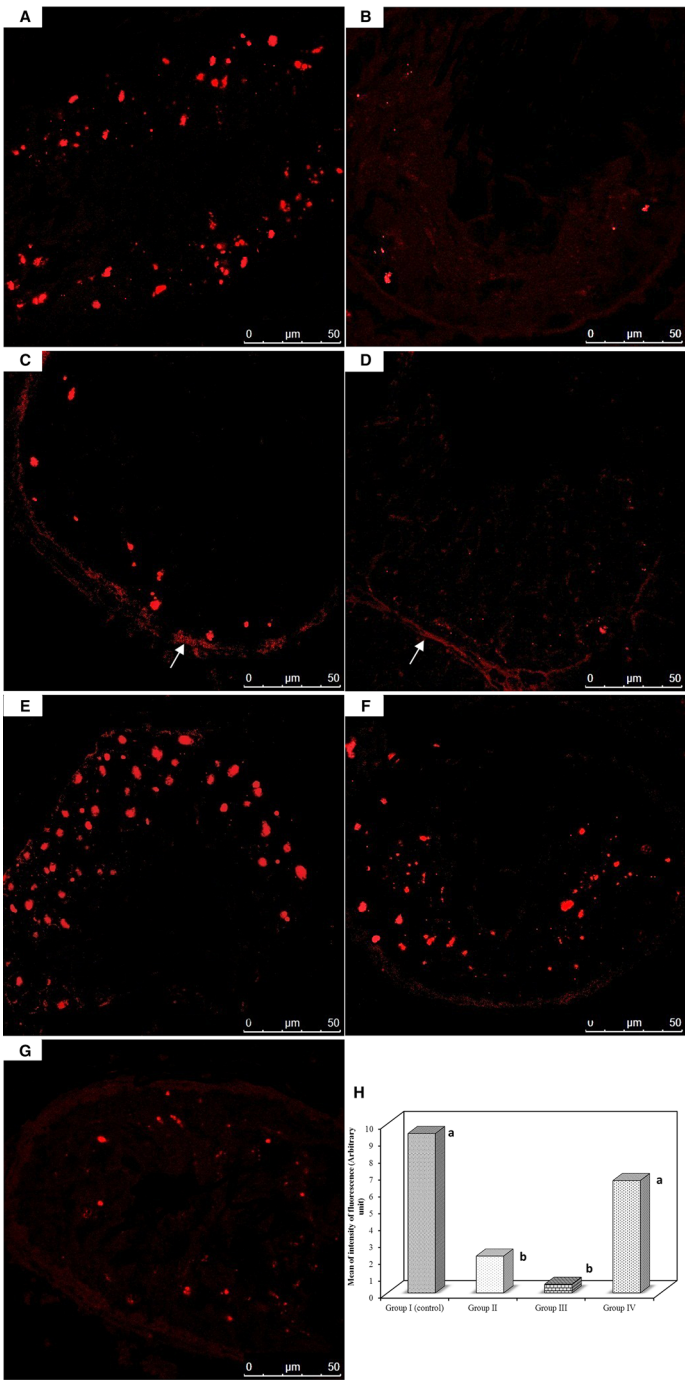

Fig. 7 Assessment of the expression of PCNA. **A** Normal expression of PCNA in the seminiferous tubules. **B**, **C** A markedly reduced immunoreactivity. **D** A minimal PCNA reaction. **E–G** Variable degrees of expression of PCNA in the seminiferous tubules. (Arrows; non-specific fluorescence of thickened basement membrane, Confocal laser scanning microscope, Original magnification X630, scale bar 50, pinhole diameter 136.9 µm). **H** Statistical comparison between the studied groups according to the intensity of fluorescence of PCNA (n = 10) values represent mean ± SD. Statistical significance was determined using ANOVA Test. Pair wise comparison between each 2 groups was done using Post Hoc Test (Tukey). Similar letters indicate no statistical difference ($p > 0.05$), while different letters indicate a true statistical difference ($p < 0.05$)

lineage. These results are in line with previous other studies [5, 11, 13].

For the transplantation procedure, we preferred the injection into the efferent ducts rather than the systemic route, as the blood-testis barrier would stop the cells from entering the testicular tissue via the circulation [46]. Furthermore, the busulfan-treated seminiferous tubules would be less resistant to the pressure of injection into the efferent ducts, due to their loosened structure [47]. Thanks to the immune privilege characteristics of the seminiferous tubules [20], and the immunosuppressive properties of the stem cells [48], the transplanted labeled AFSCs survived and homed within the testicular germinal epithelium, as proved by the confocal microscpe.

The histological examination of AFSCs-treated group, showed a great improvement of the majority of the seminiferous tubules, as evidenced by detection of the different spermatogenic cells in all stages of maturation; from spermatogonia to luminal spermatozoa. A group of studies had reported the role of MSCs from various sources in

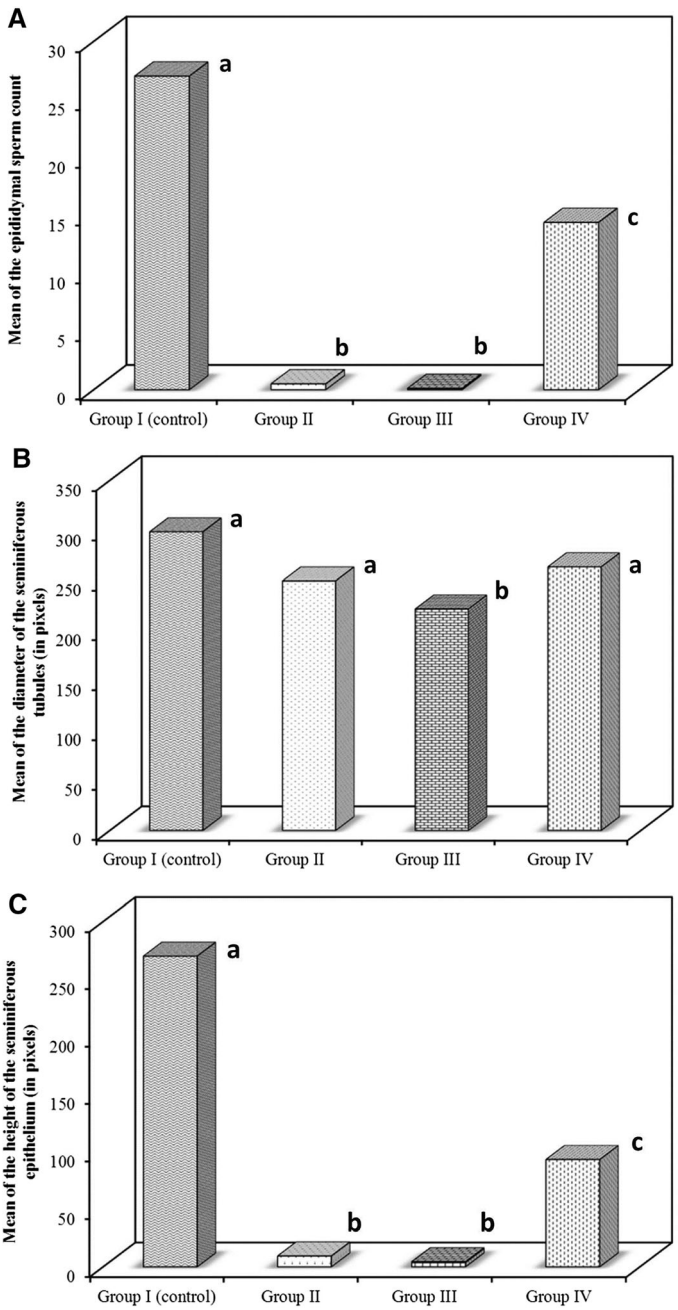

Fig. 8 Statistical comparison between the studied groups according to: **A** The epididymal sperm count (n = 10), **B** the tubular diameter (n = 25), and **C** the height of the seminiferous epithelium (n = 25): Values represent mean ± SD. Statistical significance was determined using ANOVA Test. Pair wise comparison between each 2 groups was done using Post Hoc Test (Tukey). Similar letters indicate no statistical difference ($p > 0.05$), while different letters indicate a true statistical difference ($p < 0.05$)

amelioration of busulfan-induced testicular damage, such as from; the bone marrow [19], the adipose tissue [49], and the umbilical cord [50]. However, according to our knowledge, there are no studies have investigated the possible therapeutic role of AFSCs in this concern.

The exact mechanism of action involved in stem cells therapeutic potential is still a challenge and not fully understood. There is a great discrepancy in the literature regarding this issue [51]. However, there are two main possible hypotheses that might act separately or through exerting a synergistic effect to cause the observed testicular regeneration in the AFSCs-treated group.

The first mechanism is that, AFSCs could differentiate into germ cells, as they express the embryonic marker Oct-4, at both mRNA and protein levels, just like the germ cells [52]. In addition, AFSCs harbor an interesting subpopulation of stem cells that is positive for the surface marker CD117 or c-Kit. It is a type III tyrosine kinase receptor for the stem cell factor (SCF). This marker has essential role in gametogenesis, as it is expressed on the primordial germ cells [53]. Some other researchers were on the reverse side. They stated that, differentiation of stem cells into gametes is uncommon process to happen. The transplanted cells would be unable to mimic the complex cascade of events of

differentiation of the spermatogonial stem cells, particularly after the testicular injury induced by chemotherapy [54, 55].

The second mechanism is that AFSCs could stimulate proliferation of the spermatogenic cells by secretion of massive amounts of growth factors and cytokines within extracellular vesicles (EVs). This is called "trophic or paracrine activity". AFSCs-derived EVs are immunologically inert and rapidly up-taken by the recipient cells [56]. They have several roles in limitation of damage and stimulation of tissue-intrinsic progenitors to proliferate. They are enriched with IL-6, macrophage migration inhibitory factor (MIF), stromal cell derived factor-1 (SDF-1), and several regenerative microRNAs, which exert remarkable pro-survival, anti-apoptotic and anti-inflammatory effects [57, 58].

These paracrine factors have the ability also to promote the intercellular junctions integrity, through suppression of the free radicals [59] and induction of expression of ICAM-1-N-cadherin-β-catenin protein complexes, which are crucial for cellular adhesion [39]. As a result, the inter-Sertoli junctional complexes appeared apparently intact, with normal organization of Sertoli cells upon the basement membrane in the AFSCs-treated group.

Partial regeneration and signs of residual oxidative toxic effects of busulfan were depicted in some other tubules in the AFSCs-treated group. They showed spermatozoa with electron lucent nuclei and residual excess vacuolated cytoplasm. These findings are related to busulfan-induced DNA damage, that leads to failure of chromatin condensation and failure of synthesis of the cytoskeletal proteins, resulting in impaired cytoplasmic extrusion mechanisms [60, 61].

Few seminiferous tubules in the AFSCs-treated group, were still small-sized and depleted of their spermatogenic cells. This delayed regeneration might be related to injection of insufficient amount of AFSCs, or the unequal number of cells that have entered the different tubules, during the counter-current injection into the efferent ducts [62].

In our study, we conducted an immuno-fluorescence staining procedure to detect the level of expression of PCNA in the different groups. PCNA serves as a standard marker to evaluate the state of the spermatogenic cells proliferation [63]. The results revealed qualitative and quantitative reduced expression of PCNA in the azoospermia and spontaneous recovery groups, indicating dormancy of the spermatogonial stem cells and hindering of germ cells proliferation. Several previous studies [24, 29, 30] have confirmed the ability of busulfan to deteriorate PCNA gene transcription.

After administration of the AFSCs, there was a significant increase in the PCNA expression. In agreement with our results, ALLAH SHA et al. [64] reported that, treatment with umbilical cord-MSCs caused a re-expression of PCNA in the seminiferous tubules damaged by busulfan, indicating the ability of the fetal stem cells to induce resumption of germ cells replication.

The epididymal sperm count of the different groups was parallel to the histological results. In the azoospermia and spontaneous recovery groups, we did not succeed to detect spermatozoa in most of the examined samples, in agreement with several previous investigators [17, 18, 65], due to the compromised intracellular pathways crucial for germ cells proliferation and differentiation [45]. On contrary, the epididymal sperm count demonstrated a significant increase in the AFSCs-treated group, indicating that, the transplanted cells improved the testicular microenvironment and provided the important signals that activated the spermatogenesis process and the release of the spermatozoa into the excurrent duct system [26, 30].

Regarding the histo-morphometric results, the diameter of the seminiferous tubules of the azoospermia group, was not changed significantly compared to measurements of the control group, as a result of the excess vacuolar spaces left behind the degenerated germ cells. This finding comes in correlation with Ganjalikhan-Hakemi et al. [65]. However, in the spontaneous recovery group, the diameter of the tubules decreased significantly. According to Vasiliausha SR et al. [66], this could be explained by the progressive detachment of Sertoli cells, and loss of the structural integrity of the basal compartment, leading to a sort of tubular atrophy.

Since the seminiferous tubular epithelium and its cyto-architecture is the main indicator of the normal harmonious spermatogenesis process, a quantitative measurement of the seminiferous epithelial height, was assessed. It decreased markedly in the azoospermia and spontaneous recovery groups, consequent to loss of the capacity of the germ cell to mature before being apoptotic [67]. It was improved in the AFSCs-treated group, concluding that, AFSCs ameliorated busulfan-induced apoptotic and oxidative changes, and they could be recommended as a new treatment modality for male infertility induced by chemotherapy.

Acknowledgements Authors acknowledge the technical help at the Center of Excellence for Research in Regenerative Medicine Applications (CERRMA), Alexandria Faculty of Medicine. This research received no specific grant from any funding agency in the public, commercial, or not-for-profit sectors.

Author contributions HFI carried out the experimental work, designed the experiments, and wrote the manuscript. SHS and TMZ shared in the experimental design, performed the analytical part of the study, supervised the research, and revised the manuscript. KFEM and AYM optimized the experimental design and gave a conceptual advice. All authors read and approved the manuscript.

Compliance with ethical standards

Conflict of interest The authors declared no potential conflicts of interest with respect to the research, authorship, and/or publication of this article.

Ethical statement The animal study was performed after receiving approval of the Research Ethics Committee for care and use of laboratory animals, approval No. 0201162, IRB code 00012098, FWA code 00018699, membership of Alexandria University in the International Council of Laboratory Animal Science organization (ICLAS-https://www.hhs.gov/ohrp/assurances/index.html).

References

1. Jahnukainen K, Mitchell RT, Stukenborg JB. Testicular function and fertility preservation after treatment for haematological cancer. Curr Opin Endocrinol Diabetes Obes. 2015;22:217–23.
2. Bartelink I, Lalmohamed A, van Reij EM, Dvorak CC, Savic RM, Zwaveling J, et al. A new harmonized approach to estimate busulfan exposure predicts survival and toxicity after hematopoietic cell transplantation in children and young adults: a multicenter retrospective cohort analysis. Lancet Haematol. 2016;3:e526–36.
3. Panahi S, Abdollahifar MA, Aliaghaei A, Nazarian H, Paktinat S, Abdi S, et al. Application of stereological methods for unbiased estimation of sperm morphology in the mice induced by busulfan. Anat Cell Biol. 2017;50:301–5.
4. Mahla RS. Stem cells applications in regenerative medicine and disease therapeutics. Int J Cell Biol. 2016;2016:6940283.
5. Pantalone A, Antonucci I, Guelfi M, Pantalone P, Usuelli FG, Stuppia L, et al. Amniotic fluid stem cells: an ideal resource for therapeutic application in bone tissue engineering. Eur Rev Med Pharmacol Sci. 2016;20:2884–90.
6. Loukogeorgakis SP, De Coppi P. Stem cells from amniotic fluid-Potential for regenerative medicine. Best Pract Res Clin Obstet Gynaecol. 2016;31:45–57.
7. Wen ST, Chen W, Chen HL, Lai CW, Yen CC, Lee KH, et al. Amniotic fluid stem cells from EGFP transgenic mice attenuate hyperoxia-induced acute lung injury. PLoS One. 2013;8:e75383.
8. Mun-Fun H, Ferdaos N, Hamzah SN, Ridzuan N, Hisham NA, Abdullah S, et al. Rat full term amniotic fluid harbors highly potent stem cells. Res Vet Sci. 2015;102:89–99.
9. Gholizadeh-Ghalehaziz S, Farahzadi R, Fathi E, Pashaiasl M. A mini overview of isolation, characterization and application of amniotic fluid stem cells. Int J Stem Cells. 2015;8:115–20.
10. Wang M, Li H, Si J, Dai J, Shi J, Wang X, et al. Amniotic fluid-derived stem cells mixed with platelet rich plasma for restoration of rat alveolar bone defect. Acta Biochim Biophys Sin (Shanghai). 2017;49:197–207.
11. Al-Husseiny F, Sobh MA, Ashour RH, Foud S, Medhat T, El-Gilany AH, et al. Amniotic fluid-derived mesenchymal stem cells cut short the acuteness of cisplatin-induced nephrotoxicity in Sprague–Dawley rats. Int J Stem Cells. 2016;9:70–8.
12. Katsares V, Petsa A, Felesakis A, Paparidis Z, Nikolaidou E, Gargani S, et al. A rapid and accurate method for the stem cell viability evaluation: the case of the thawed umbilical cord blood. Lab Med. 2015;40:557–60.
13. Thilakavathy K, Nordin N, Ramasamy R, Ghoraishizadeh P, Rohayu IM, Singh G. Characteristics of full-term amniotic fluid-derived mesenchymal stem cells in different culture media. In: Pham PV, editor. Mesenchymal stem cells: isolation, characterization and applications. Croatia: IntechOpen; 2017. p. 39–54.
14. Pochampally R. Colony forming unit assays for MSCs. Methods Mol Biol. 2008;449:83–91.
15. Molecular Probes. DiI Derivatives for Long-Term Cellular Labeling. 2005. https://assets.thermofisher.com/TFS-Assets/LSG/manuals/mp06999.pdf. Accessed July 2020.
16. BioTek. Sample preparation for fluorescence microscopy: an introduction. Concepts and tips for better fixed sample imaging results. 2015. https://www.biotek.com/resources/white-papers/sample-preparation-for-fluorescence-microscopy-an-introduction-concepts-and-tips-for-better-fixed-sample-imaging-results/. Accessed July 2020.
17. Ghasemzadeh-Hasankolaei M, Batavani R, Eslaminejad MB, Sayahpour F. Transplantation of autologous bone marrow mesenchymal stem cells into the testes of infertile male rats and new germ cell formation. Int J Stem Cells. 2016;9:250–63.
18. Jafarian A, Lakpour N, Sadeghi MR, Salehkhou S, Akhondi MM. Transplantation of spermatogonial stem cells suspension into rete testis of azoospermia mouse model. Urol J. 2018;15:40–7.
19. Tamadon A, Mehrabani D, Rahmanifar F, Jahromi AR, Panahi M, Zare S, et al. Induction of spermatogenesis by bone marrow-derived mesenchymal stem cells in busulfan-induced azoospermia in hamster. Int J Stem Cells. 2015;8:134–45.
20. Ghasemzadeh-Hasankolaei M, Eslaminejad MB, Sedighi-Gilani M. Derivation of male germ cells from ram bone marrow mesenchymal stem cells by three different methods and evaluation of their fate after transplantation into the testis. In Vitro Cell Dev Biol Anim. 2016;52:49–61.
21. Bilinska B, Hejmej A, Kotula-Balak M. Preparation of testicular samples for histology and immunohistochemistry. Methods Mol Biol. 2018;1748:17–36.
22. Dykstra MJ. Specimen preparation. In: Michael JD, editor. A Manual of applied techniques for biological electron microscopy. 4th ed. New York: Plenum Press; 2017. p. 1–18.
23. Du Z, Xu S, Hu S, Yang H, Zhou Z, Sidhu K, et al. Melatonin attenuates detrimental effects of diabetes on the niche of mouse spermatogonial stem cells by maintaining Leydig cells. Cell Death Dis. 2018;9:968.
24. Levi M, Stemmer SM, Stein J, Shalgi R, Ben-Aharon I. Treosulfan induces distinctive gonadal toxicity compared with busulfan. Oncotarget. 2018;9:19317–27.
25. Tajaddini S, Ebrahimi S, Behnam B, Bakhtiyari M, Joghataei MT, Abbasi M, et al. Antioxidant effect of manganese on the testis structure and sperm parameters of formalin-treated mice. Andrologia. 2014;46:246–53.
26. Rahmanifar F, Tamadon A, Mehrabani D, Zare S, Abasi S, Keshavarz S, et al. Histomorphometric evaluation of treatment of rat azoospermic seminiferous tubules by allotransplantation of bone marrow-derived mesenchymal stem cells. Iran J Basic Med Sci. 2016;19:653–61.
27. Wen Q, Wang Y, Tang J, Cheng CY, Liu YX. Sertoli cell Wt1 regulates peritubular myoid cell and fetal Leydig cell differentiation during fetal testis development. PLoS One. 2016;11:e0167920.
28. Kotz S, Read CB, Balakrishnan N, Vidakovic B, Johnson NL. Encyclopedia of statistical sciences. 2nd ed. Hoboken, New Jersey: Wiley-Interscience; 2006.
29. Chen X, Liang M, Wang D. Progress on the study of the mechanism of busulfan cytotoxicity. Cytotechnology. 2018;70:497–502.
30. Aboul Fotouh GI, Abdel-Dayem MM, Ismail DI, Mohamed HH. Histological study on the protective effect of endogenous stem cell mobilization in busulfan-induced testicular injury in albino rats. J Microsc Ultrastruct. 2018;6:197–204.
31. Ghadially FN. Ultrastructural pathology of the cell and matrix: a text and atlas of physiological and pathological alterations in the

fine structure of cellular and extracellular components. 3rd ed. New York: Elsevier; 2013.
32. Iwamoto T, Hiraku Y, Oikawa S, Mizutani H, Kojima M, Kawanishi S. DNA intrastrand cross-link at the 50-GA-30 sequence formed by busulfan and its role in the cytotoxic effect. Cancer Sci. 2004;95:454–8.
33. Furukawa S, Usuda K, Abe M, Hayashi S, Ogawa I. Busulfan-induced apoptosis in rat placenta. Exp Toxicol Pathol. 2007;59:97–103.
34. Gutierrez K, Glanzner WG, Chemeris RO, Rigo ML, Comim FV, Bordignon V, et al. Gonadotoxic effects of busulfan in two strains of mice. Reprod Toxicol. 2016;59:31–9.
35. Qin Y, Liu L, He Y, Ma W, Zhu H, Liang M, et al. Testicular injection of busulfan for recipient preparation in transplantation of spermatogonial stem cells in mice. Reprod Fertil Dev. 2016;28:1916–25.
36. Bahmanpour S, Namavar Jahromi B, Koohpeyma F, Keshavarz M, Bakhtari A. Effects of different doses and time-dependency of busulfan on testes parameters and spermatogenesis in a rat model: a quantitative stereological study. JAMSAT. 2017;3:155–62.
37. Cai Y, Liu T, Fang F, Shen S, Xiong C. Involvement of ICAM-1 in impaired spermatogenesis after busulfan treatment in mice. Andrologia. 2016;48:37–44.
38. Fang F, Ni K, Cai Y, Zhao Q, Shang J, Zhang X, et al. Busulfan administration produces toxic effects on epididymal morphology and inhibits the expression of ZO-1 and vimentin in the mouse epididymis. Biosci Rep. 2017;37:BSR20171059.
39. Cai YT, Xiong CL, Shen SL, Rao JP, Liu TS, Qiu F. Mesenchymal stem cell-secreted factors delayed spermatogenesis injuries induced by busulfan involving intercellular adhesion molecule regulation. Andrologia. 2019;51:e13285.
40. Li B, He X, Zhuang M, Niu B, Wu C, Mu H, et al. Melatonin ameliorates busulfan-induced spermatogonial stem cell oxidative apoptosis in mouse testes. Antioxid Redox Signal. 2018;28:385–400.
41. Mitchell RN. The cell as a unit of health and disease. In: Kumar V, Abbas AK, Aster JC, editors. Robbins and cotran pathologic basis of disease. 10th ed. New York: Elsevier Health Sciences; 2018. p. 1–30.
42. Meligy FY, Abo Elgheed AT, Alghareeb SM. Therapeutic effect of adipose-derived mesenchymal stem cells on Cisplatin induced testicular damage in adult male albino rat. Ultrastruct Pathol. 2019;43:28–55.
43. Sasso-Cerri E, Oliveira B, de Santi F, Beltrame FL, Caneguim BH, Cerri PS. The antineoplastic busulphan impairs peritubular and Leydig cells, and vitamin B12 stimulates spermatogonia proliferation and prevents busulphan-induced germ cell death. Biomed Pharmacother. 2017;95:1619–30.
44. Qu N, Itoh M, Sakabe K. Effects of chemotherapy and radiotherapy on spermatogenesis: the role of testicular immunology. Int J Mol Sci. 2019;20:957.
45. Anand S, Bhartiya D, Sriraman K, Mallick A. Underlying mechanisms that restore spermatogenesis on transplanting healthy niche cells in busulphan treated mouse testis. Stem Cell Rev Rep. 2016;12:682–97.
46. Atalla S, Saleh H, Abdel Gawad S, Mohamed H. Histological study on the effect of adipose tissue-derived mesenchymal stem cells on the testis of chemically induced castration model by calcium chloride in adult albino rats. Egypt J Histol. 2017;40:486–96.
47. Hajihoseini M, Vahdati A, Ebrahim Hosseini S, Mehrabani D, Tamadon A. Induction of spermatogenesis after stem cell therapy of azoospermic guinea pigs. Vet Arh. 2017;87:333–50.
48. Aghamir SM, Salavati A, Yousefie R, Tootian Z, Ghazaleh N, Jamali M, et al. Does bone marrow-derived mesenchymal stem cell transfusion prevent antisperm antibody production after traumatic testis rupture? Urology. 2014;84:82–6.
49. Mehrabani D, Hassanshahi MA, Tamadon A, Zare S, Keshavarz S, Rahmanifar F, et al. Adipose tissue-derived mesenchymal stem cells repair germinal cells of seminiferous tubules of busulfan-induced azoospermic rats. J Hum Reprod Sci. 2015;8:103–10.
50. Chen H, Tang QL, Wu XY, Xie LC, Lin LM, Ho GY, et al. Differentiation of human umbilical cord mesenchymal stem cells into germ-like cells in mouse seminiferous tubules. Mol Med Rep. 2015;12:819–28.
51. Mastrolia I, Foppiani EM, Murgia A, Candini O, Samarelli AV, Grisendi G, et al. Challenges in clinical development of mesenchymal stromal/stem cells: concise review. Stem Cells Transl Med. 2019;8:1135–48.
52. Xiao GY, Liu IH, Cheng CC, Chang CC, Lee YH, Cheng WT, et al. Amniotic fluid stem cells prevent follicle atresia and rescue fertility of mice with premature ovarian failure induced by chemotherapy. PLoS One. 2014;9:e106538.
53. Antonucci I, Pantalone A, Tete S, Salini V, Borlongan CV, Hess D, et al. Amniotic fluid stem cells: a promising therapeutic resource for cell-based regenerative therapy. Curr Pharm Des. 2012;18:1846–63.
54. de Sousa Lopes SC, Roelen BA. Current status of in vitro differentiation of stem cells into gametes. Anim Reprod. 2018;12:46–51.
55. Zhang D, Liu X, Peng J, He D, Lin T, Zhu J, et al. Potential spermatogenesis recovery with bone marrow mesenchymal stem cells in an azoospermic rat model. Int J Mol Sci. 2014;15:13151–65.
56. Balbi C, Piccoli M, Barile L, Papait A, Armirotti A, Principi E, et al. First characterization of human amniotic fluid stem cell extracellular vesicles as a powerful paracrine tool endowed with regenerative potential. Stem Cells Transl Med. 2017;6:1340–55.
57. Balbi C, Lodder K, Costa A, Moimas S, Moccia F, van Herwaarden T, et al. Reactivating endogenous mechanisms of cardiac regeneration via paracrine boosting using the human amniotic fluid stem cell secretome. Int J Cardiol. 2019;287:87–95.
58. Morigi M, De Coppi P. Cell therapy for kidney injury: different options and mechanisms-mesenchymal and amniotic fluid stem cells. Nephron Exp Nephrol. 2014;126:59.
59. Abdelaziz MH, Salah El-Din EY, El-Dakdoky MH, Ahmed TA. The impact of mesenchymal stem cells on doxorubicin-induced testicular toxicity and progeny outcome of male prepubertal rats. Birth Defects Res. 2019;111:906–19.
60. Rajesh Kumar T, Doreswamy K, Shrilatha B. Oxidative stress associated DNA damage in testis of mice: induction of abnormal sperms and effects on fertility. Mutat Res. 2002;513:103–11.
61. Malekinejad H, Mirzakhani N, Razi M, Cheraghi H, Alizadeh A, Dardmeh F. Protective effects of melatonin and Glycyrrhiza-glabra extract on ochratoxin. A-induced damages on testes in mature rats. Hum Exp Toxicol. 2011;30:110–23.
62. Monsefi M, Fereydouni B, Rohani L, Talaei T. Mesenchymal stem cells repair germinal cells of seminiferous tubules of sterile rats. Iran J Reprod Med. 2013;11:537–44.
63. Zhao WP, Wang HW, Liu J, Tan PP, Luo XL, Zhu SQ, et al. Positive PCNA and Ki-67 expression in the testis correlates with spermatogenesis dysfunction in fluoride-treated rats. Biol Trace Elem Res. 2018;186:489–97.
64. Allah SH, Pasha HF, Abdelrahman AA, Mazen NF. Molecular effect of human umbilical cord blood CD34-positive and CD34-negative stem cells and their conjugate in azoospermic mice. Mol Cell Biochem. 2017;428:179–91.
65. Ganjalikhan-Hakemi S, Sharififar F, Haghpanah T, Babaee A, Eftekhar-Vaghefi SH. The effects of olive leaf extract on the

testis, sperm quality and testicular germ cell apoptosis in male rats exposed to busulfan. Int J Fertil Steril. 2019;13:57–65.
66. Vasiliausha SR, Beltrame FL, de Santi F, Cerri PS, Caneguim BH, Sasso-Cerri E. Seminiferous epithelium damage after short period of busulphan treatment in adult rats and vitamin B12 efficacy in the recovery of spermatogonial germ cells. Int J Exp Pathol. 2016;97:317–28.
67. Hejazi S. Toxicity effect of cisplatin –treatment on rat testis tissue. J Mens Health. 2011;8:235.